molecular pharmaceutics

Review

pubs.acs.org/molecularpharmaceutics

From PET/CT to PET/MRI: Advances in Instrumentation and Clinical Applications

Zhenhua Hu,[†,§] Weidong Yang,[‡,§] Haixiao Liu,[†,§] Kun Wang,[†,§] Chengpeng Bao,[†] Tianming Song,[†] Jing Wang,*[,‡] and Jie Tian*[,†]

[†]Institute of Automation, Chinese Academy of Sciences, Beijing 100190, China

[‡]Department of Nuclear Medicine, Xijing Hospital, Fourth Military Medical University, Xi'an 710032, China

ABSTRACT: Multimodality imaging of positron emission tomography/computed tomography (PET/CT) provides both metabolic information and the anatomic structure, which is significantly superior to either PET or CT alone and has greatly improved its clinical applications. Because of the higher soft-tissue contrast of magnetic resonance imaging (MRI) and no extra ionizing radiation, PET/MRI imaging is the hottest topic currently. PET/MRI is swiftly making its way into clinical practice. However, it has many technical difficulties to overcome, such as photomultiplier tubes, which cannot work properly in a magnetic field, and the inability to provide density information on the object for attenuation correction. This paper introduces the technique process of PET/MRI and summarizes its clinical applications, including imaging in oncology, neurology, and cardiology.

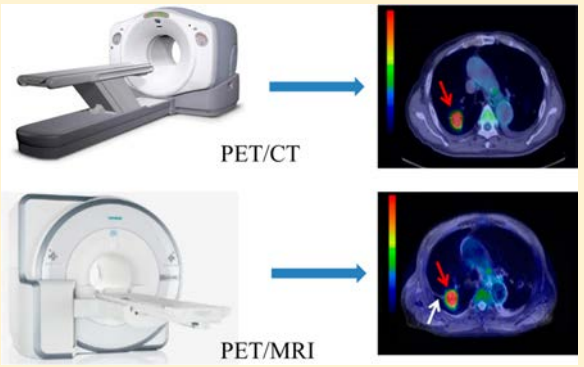

KEYWORDS: *positron emission tomography/computed tomography (PET/CT), positron emission tomography/magnetic resonance imaging (PET/MRI), time-of-flight (TOF), silicon photomultiplier (SiPM), attenuation correction, oncology, neurologic disease, cardiology*

1. INTRODUCTION

Positron emission tomography (PET) can provide functional information on biological tissues and molecular information on biological processes by the use of radiopharmaceuticals, which have been widely used in preclinical and clinical applications.[1−4] As a functional imaging technology, PET can give precise metabolic information but does not provide clear visualization of anatomical structures, which is its major limitation. Hybrid positron emission tomography/computed tomography (PET/CT) imaging provides both metabolic information and the anatomical structure by combining PET and CT, making this method significantly superior to either PET or CT alone and greatly improving its clinical outcomes. PET/CT has been used heavily in clinical oncology, neurology, and cardiology. It is also an important research scanner in human brain mapping, heart function studies, and drug developments.

Magnetic resonance imaging (MRI), another anatomical imaging modality, is superior to CT in providing high-resolution anatomical information with excellent soft-tissue contrast. One of the major advantages of MRI compared with CT is the fact that it is radiation-free, thus allowing patients to undergo multiple scans without concerns about excessive radiation dose, especially in monitoring therapy or scanning pediatrics. For these reasons, combining PET and MRI has become a topic of discussion in the imaging community over the past several years. Because of the strong magnetic field produced by MRI, the combination of PET and MRI is a challenging problem, and many efforts have been devoted to solving it. The sequential PET/MRI system scans the PET and MRI images on two devices separately to avoid the interaction of the two systems. The simultaneous PET/MRI system combines the two modalities by a total redesign of the PET detector to be compatible with the MRI device. For PET/MRI, another challenge is that the MRI cannot provide information on electron density, which can be converted to the attenuation coefficient used for attenuation correction. As a result, the quality of the PET image is decreased compared with that obtained using PET/CT. The solution of this problem is still not satisfactory. The main solution is to segment the MRI image to obtain the attenuation coefficient map. However, bones cannot be segmented accurately from conventional MRI images, and thus, an accurate attenuation coefficient map is still difficult to obtain.

Presently, the dual-modality PET/MRI technique has been applied in preclinical studies and clinics. The resulting combination of molecular, functional, and morphological information is paving the way for a better understanding of

Special Issue: Positron Emission Tomography: State of the Art

Received: April 30, 2014
Revised: July 18, 2014
Accepted: July 24, 2014
Published: July 24, 2014

Table 1. Comparison of Commercially Available Whole-Body PET/MRI Systems

company	GE	Philips	Siemens
model	Discovery PET/CT+MR combo	Ingenuity TF PET/MR	Biograph mMR
scan scheme	sequential	sequential	simultaneous
mode	time-of-flight	time-of-flight	conventional
inner bore dimensions	70 cm	PET, 70 cm; MR, 60 cm	60 cm
system sensitivity	7.5 cps kBq	7 cps kBq	13.2 cps kBq
transverse resolution	4.0 mm	4.9 mm	4.4 mm
axial resolution	5.0 mm	4.9 mm	4.5 mm

molecular biology details, disease mechanisms, and pharmacokinetics in animals and humans. In this paper, we introduce the technique process of PET/MRI and summarize its clinical applications, including tumor, neuro-, and cardiac imaging.

2. ADVANCES IN PET SYSTEMS

2.1. PET. In PET imaging, a positron-labeled probe is injected intravenously into the patient, is distributed throughout the body via the bloodstream, and enters the organs.[5] PET imaging is performed on the patient 40 min after the vein injection of the nuclear probes. As the radioisotope undergoes positron emission decay, a positron is emitted from the nucleus and travels in tissues for a short distance before being annihilated. When the positron meets an electron, annihilation occurs, and a pair of annihilation γ photons move in approximately opposite directions. γ photons are emitted from the surface of the human body and can be detected by the PET system.

PET imaging utilizes a dedicated PET camera system that includes multiple rings of detectors. Similar to γ cameras, PET detectors consist of scintillation crystals coupled with photomultiplier tubes (PMTs). The scintillation crystals used in clinical PET imaging are either bismuth germanium oxide (BGO), gadolinium oxyorthosilicate (GSO), or lutetium oxyorthosilicate (LSO).

Presently, the most advanced clinical PET scanners can offer spatial resolution with the limitation around 4^3 mm^3. The sensitivity varies between 10^{-11} and 10^{-12} mol/liter, which is independent of the location depth of the tracer of interest.

For human imaging, time-of-flight (TOF) PET information provides better localization of the annihilation event along the line of the response, resulting in an overall improvement in the signal-to-noise ratio (SNR) of the reconstructed image. The SNR can be improved by constraining the annihilation position by using timing information.

2.2. PET/CT. As an imaging technique, PET provides functional information with limited spatial resolution.[6] To overcome this limitation, the combination of a PET scanner and a CT scanner in a single dual-modality PET/CT system has been widely applied in clinics to acquire nuclear images with high-resolution structural information. CT can provide anatomical information on tissues and organs in three-dimensional (3D) viewing, which offers excellent complementarity for monomodal PET. In clinics, 64-slice PET/CT is a highly precise and revolutionary metabolic imaging technique. It simplifies complicated high-end work and makes diagnosis of cancer and other lesions more accurate.[7] However, the significant extra radiation and low soft-tissue contrast from CT also limits its clinical applications.[8−10]

2.3. PET/MRI. PET/CT is a milestone in molecular imaging and has been widely used in clinical cancer diagnosis. However, for applications requiring high soft-tissue contrast and low radiation doses, PET/MRI is more qualified. In a PET/MRI system, MRI provides the structural information with high spatial resolution and soft-tissue contrast while PET provides the physiological and metabolic information at the cellular level. The combination of the two modalities contributes great advantages in oncologic, neurologic, and cardiovascular imaging.[11−13] Compared with the PET/CT system, PET/MRI is a newer technology and not widely spread in the market, but it has many advantages:[14,15]

(1) Unlike CT, MRI does not bring in any ionizing radiation. Therefore, PET/MRI is more suitable for pediatric imaging, where the radiation dose is strictly controlled. Especially in cases where continuous monitoring of treatment progress is necessary, this superiority is even more significant.[14]

(2) MRI has excellent soft-tissue contrast and the ability to manipulate tissue contrast through a variety of imaging sequences. Therefore, PET/MRI is better than PET/CT for imaging of complicated heterogeneous tissue environments, such as the brain and liver, without using a contrast medium.

(3) Both MRI and PET have advanced functional and molecular imaging capacity. With suitable molecular imaging probes, PET/MRI can offer more comprehensive physiological and pathological information at the cellular and molecular levels.

(4) In the state-of-the-art PET/MRI design, MRI and PET can acquire data simultaneously. As a consequence, anatomical, metabolic, and even molecular information can be observed at the same time for an imaging subject in PET/MRI. PET/CT, however, can acquire data only sequentially, with the challenge of accurate imaging registration.

2.3.1. System Design. With the advantages listed above, PET/MRI has attracted much attention in recent years.[16−19] Many efforts have been devoted to combining the two modalities without compromising the imaging quality. The development of PET/MRI systems can be briefly categorized into small-animal PET/MRI, brain PET/MRI, and whole-body PET/MRI. This paper mainly discusses whole-body PET/MRI. The three major commercial whole-body PET/MRI systems are listed in Table 1. MRI generates a strong magnetic field and causes an interaction with the PET system, which leads to quality degradation of both modalities. To solve this problem, two major design concepts of whole-body PET/MRI have been proposed: sequential scanning and simultaneous scanning.

Scanning PET and MRI sequentially is the most straightforward idea for constructing a PET/MRI system. In a sequential PET/MRI system, PET and MRI scans are performed sequentially on two distinct systems as part of a single examination.[20] The sequential system is relatively easy to establish because of the small extent of interaction between PET and MRI. The major examples of sequential PET/MRI are General Electric (GE) Healthcare's Discovery PET/CT+MR combo and Philips Healthcare's Ingenuity TF system.[21,22] A

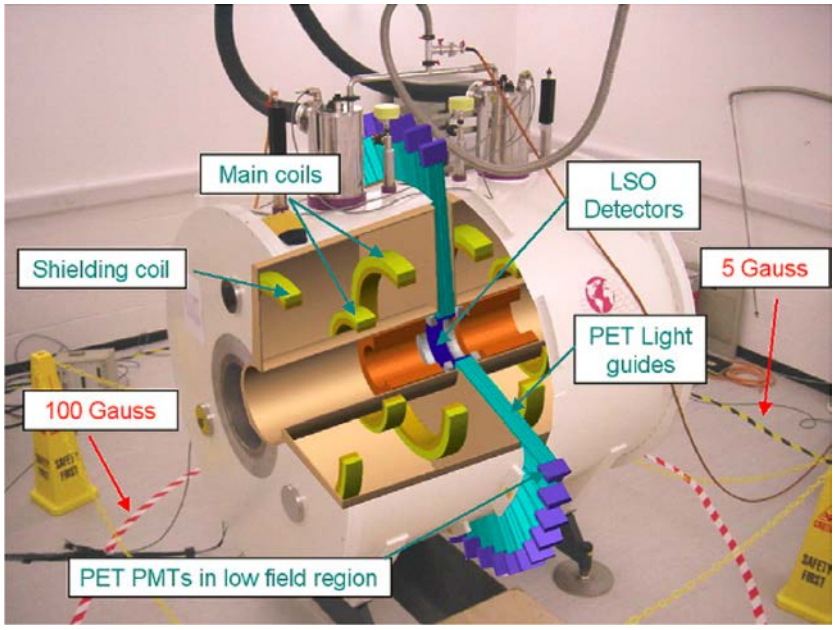

Figure 1. Simultaneous PET/MRI system adopts fibers (light guides) to transmit the photons emitted from the scintillation crystal and places the PMTs far away from the magnetic field. The magnet is split to make space for the PET detector and fibers.[32]

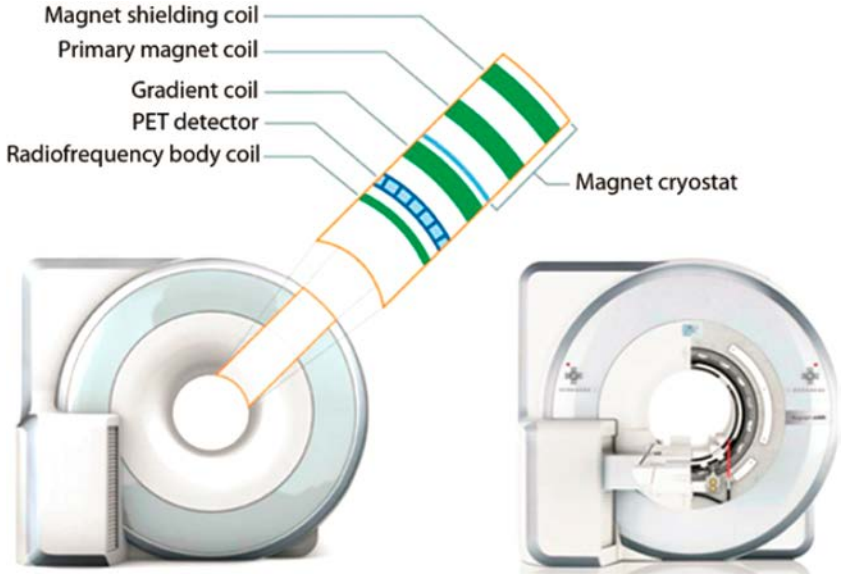

Figure 2. Sectional view of the Siemens Biograph mMR, the first fully integrated simultaneous PET/MRI system. The PET detector is placed between the radiofrequency coil and the gradient coil.[32]

patient bed compatible with both modalities brings the PET and MRI devices together.[22] The difference between the two designs is whether the two systems are in the same room. The Philips Healthcare's design puts the two systems in the same room. The patient bed can rotate 180° to get the patient into the two systems sequentially. A rather big room is needed to place the two systems far enough apart to reduce their interaction. The GE design places the two systems in separate rooms. The patient is transferred from one scanner room to the other on a specially designed patient bed. The quality of the images remains nearly the same compared with a single modality because of adequate distance and some bulky shielding.[23] The images obtained by the two modalities are registered by software according to the sensor-coded bed position. The advantage of this design is that PET and MRI can operate separately when the patient does not need dual-modality information. The system is flexible according to the application and workload, but as the two modalities are scanned at different time points, it is difficult to guarantee that the posture and metabolic state of the patient are the same. The resulting difficulties depend on the registration restrictions of the system in some special applications. It is noteworthy that the two models from GE and Philips have a major difference. The Discovery PET/CT+MR combo system needs CT information to conduct an attenuation correction of the PET data, so excessive radiation is still needed. In contrast, the Ingenuity TF system adopts an MRI-based attenuation correction.

In order to overcome the disadvantages of the sequential system, simultaneous PET/MRI systems have been designed.

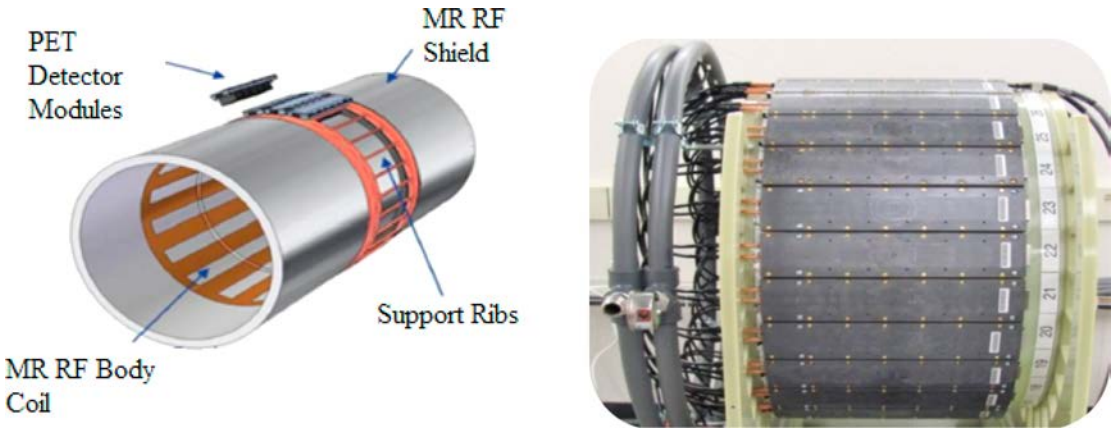

Figure 3. Structure of the GE Signa, the first integrated-TOF simultaneous PET/MRI system. Image courtesy of GE Healthcare.

Simultaneous PET/MRI systems are expected to offer structural and functional scanning at the same time. Unlike sequential systems, for simultaneous PET/MRI systems the interaction problem is solved by totally redesigning the structures of the PET and MRI systems. The major interaction problems of simultaneous PET/MRI are the following: (1) the PMT used in the PET system cannot work properly in the magnetic field of the MRI system; (2) the PET photodetector may interfere with the radiofrequency (RF) and gradient coils, resulting in a nonuniform magnetic field; (3) an eddy current may occur if metallic shielding is used.[24] Many prototype PET/MRI systems were developed to overcome these problems. In the early designs, researchers used PET detectors based on traditional PMTs.[25−28] Usually, these kinds of simultaneous PET/MRI systems adopted fibers to transmit photons emitted from the scintillation crystal and placed the PMTs far away from the magnetic field (Figure 1). However, photon loss in the fibers led to a substantial degradation of the energy resolution at the photopeak.[29] Other groups used magnetically immune photomultipliers, such as avalanche photodiodes (APDs) and silicon photomultipliers (SiPMs), as substitutes for PMTs. APDs are magnetically immune. Compared with a PMT, an APD not only has a higher quantum efficiency but also requires a lower supply voltage. Moreover, the small size of an APD makes a PET detector easy to integrate with MRI. All of those characteristics make APDs very suitable for simultaneous PET/MRI. Besides the advantages of APDs, SiPMs have better time resolution and magnetic immunity.[30] Siemens Healthcare (Erlangen, Germany) developed the first whole-body simultaneous PET/MR system (Magnetom Biograph mMR), which used APDs to avoid interference from the magnetic fields. The PET detector was placed between the RF coil and the gradient coil (Figure 2). This was the first time that one system could conduct whole-body PET and MRI scans coaxially and simultaneously. In this PET/MRI system, the MRI subsystem consisted of a 3.0 T niobium−titanium superconductor magnet, an actively shielded whole-body gradient coil with an amplitude of 45 mT/m, and an RF body coil with a transmitter bandwidth of 800 MHz. The magnetic-field-compatible PET detector consisted of 56 detector blocks. Each detector block was composed of 64 LSO scintillation crystals and nine APDs. Recent reports have proved that the interference between PET and MRI in the Biograph mMR instrument is insignificant.[31,32] The Biograph mMR system has been applied in diagnosis of prostate cancer, breast cancer, and so on.[33,34] Furthermore, the performance of this system has been compared with PET/CT.[33−35] Despite the advantages of this cutting-edge design, some drawbacks still exist. The radius of the RF coil is reduced to provide space for the PET detector, which leads to a decrease in the field of view (FOV). Additionally, the PET detector does not have TOF capability because of the low time resolution of APDs.

Compared with a conventional PET/MRI system, a PET/MRI system with TOF technology can significantly improve the spatial resolution, reduce the dose of radiation, and enhance the precision of attenuation corrections. Because of these advantages, integrated-TOF whole-body PET/MRI has presently been a hot research topic. GE Healthcare developed a prototype integrated-TOF whole-body PET/MRI instrument, Signa, in 2013. In this system, the PET detector consists of an LBS scintillation crystal and SiPM and has a sensitivity of 23 cps kBq and an FOV of 25.06 cm. SiPMs have good timing performance, which makes them perfect for integrated-TOF PET/MRI.[30] The MRI subsystem employs a novel transparent surface coil, and the intensity of the magnetic field is 3.0 T. The MRI works in a sequence of LAVA flex + STIR + PROPELLER T2 to conduct the MR-based attenuation correction. Compared with Biograph mMR, the GE Signa system has many advantages. First, the injection dose is reduced by 75% through the introduction of TOF technology. Second, the novel transparent surface coil reduces the interaction and improves the imaging quality. Third, the PET detector is inserted into the RF coil, so the bores of the PET and MRI subsystems are the same size (Figure 3). This is convenient for postregistration and fusion. Furthermore, the design also avoids the diminution of the RF coils and leads to a bigger FOV, which is 33% larger than in the Biograph mMR system. This design is awaiting FDA approval and may soon be available commercially. Philips also has an TOF PET/MRI research project underway, which has been reported to have accurate depth-of-interaction (DOI) correction technology (http://www.sublima-pet-mr.eu/).

Although an integrated-TOF PET/MRI system has been developed, there are still many problems to be solved. A large number of SiPMs and conversion circuits are needed for simultaneous TOF PET/MRI, which makes the instrument expensive to use. Besides, TOF PET/MRI has similar problems as PET/MRI, such as the dual-modality imaging probes and clinic workflow, which need to be developed for further application.[36] Optimized scan protocols for different applications should be developed. The associated risk and the elimination of prejudice should be tested further.[37]

2.3.2. Attenuation Correction. After the PET/MRI scan, the MRI and PET images are fused by software. The MRI image is used to provide the location information and conduct the attenuation correction of the PET image. Many MRI-based attenuation correction methods have been established in recent years.

When a γ photon travels in the medium, there is a possibility that it will be absorbed or scattered by an atom. Thus, the deeper it is inside the body, the larger is this possibility, and the useful signal detected by the PET detector is diminished, causing a decline in the quality of the image. Attenuation correction deals with this problem. Among all of the attenuation correction methods, the most important part is to obtain the attenuation map, which is the distribution of the attenuation coefficient (usually called the μ value).[38] The attenuation coefficient is associated with the electron density of the tissue. CT image values are also related to electron density and can be converted into 511 keV attenuation maps. However, the attenuation map cannot be obtained directly from the MRI image, which is associated with the hydrogen ion density and relaxation time. Therefore, attenuation correction is a challenge for PET/MRI. At present, the attenuation correction methods for PET/MRI are mainly atlas-based, segment-based, transmission-based, or emission-based.

The atlas-based method usually uses a pattern recognition algorithm to match the MR image to an atlas of MRI−CT data sets to obtain an attenuation map.[39] This method provides a continuous attenuation coefficient and does not need additional acquisition time. However, the method relies on a reference date, which brings in some uncertainty. The MR coil's attenuation is also ignored. The segment-based method is the most common method in attenuation correction for PET/MRI. The MR image is segmented into different organs to assign the corresponding experiential attenuation coefficients, so an accurate attenuation map needs to be able to segment at least five tissues: air, lungs, soft tissues, spongy bone, and cortical bone.[38] The segment between cortical bone and air is a challenge. The conventional-sequence MRI image cannot provide a contrast between cortical bone and air. The cortical bone is ignored and assigned the attenuation coefficient of soft tissue in the Dixon-based method.[40] Andersen et al.[19] have proven that ignoring cortical bone results in errors of up to 31.0% for bony regions. The ultrashort echo time (UTE) sequence is adopted to distinguish cortical bone from air in brain MRI.[41] The UTE sequence is time-consuming and has a small FOV, which prevents its application on whole-body PET/MRI. Furthermore, to assign a corresponding experiential attenuation coefficient also introduces some error because of the interpatient variability of attenuation coefficients.[42] The transmission-based method usually places a fixed positron-emitting transmission source inside the FOV. The transmission image is used to obtain the attenuation map, while the emission image is used to reconstruct the distribution of the tracer. The additional scan of the transmission image usually requires additional acquisition time.[43] Therefore, emission and transmission imaging is expected to be scanned at the same time. Mollet et al.[44] provided a transmission-based method that uses a static annulus-shaped transmission source. This method solves most of the problems related to atlas-based and segment-based attenuation correction. The method takes advantage of the TOF data to distinguish the emission signal from the transmission signal, which leads to the unfitness of the PET/MRI system without TOF technology. Further study based on integrated-TOF whole-body PET/MRI is still needed. The emission-based method tries to reconstruct the distribution of the tracer and the attenuation map simultaneously from one PET scan. The problem is underdetermined, and some constraint is introduced to solve the problem. The maximum-likelihood reconstruction of attenuation and activity (MLAA) was established by taking into account the Poisson nature of the data.[45] Another study used this method for truncation artifact correction.[46] By inclusion of the TOF data, the TOF-MLAA obtained the attenuation sonogram up to a constant[47] and reduced the quantitative bias.[48] The main problem of this method is that the attenuation map is noisy because of the crosstalk between the emission and transmission. In conclusion, MR-based attenuation correction still needs development and clinical testing.

3. CLINICAL APPLICATIONS OF PET TECHNOLOGY

3.1. Clinical Applications of PET/CT. PET, as a functional imaging technology, can provide precise metabolic information, but its inability to provide clear anatomical structure is its major limitation. Hybrid PET/CT imaging provides both metabolic information and the anatomical structure by combining PET and CT. It is significantly superior to either PET or CT alone and can greatly improve the clinical applications of PET. PET/CT can detect the metabolic differences between tissues with various radiotracers, such as ^{18}F-FDG, ^{18}F-FLT, and so on. FDG is a glucose analogue that has a similar cellular uptake as glucose but can be metabolically trapped within the cell after enzymatic phosphorylation to FDG-6-phosphate. Since malignant cells grow significantly faster and can take up more ^{18}F-FDG than normal cells do, ^{18}F-FDG PET/CT scanning is a popular method for tumor imaging and has been proven to be an important tool for tumor diagnosis. It is essential in medicine, where more than 95% of PET scans used for tumors include diagnosis, staging, and therapy monitoring. Since its foundation at the beginning of the century, millions of patients have undergone PET or PET/CT scans for thousands of publications; many papers have been widely reviewed for their clinical applications in various diseases (diagnosis, staging, and therapy monitoring of tumors, evaluation of the survival of the myocardium, exploration of the function of the nervous system, etc.). Therefore, it is not necessary for us to repeatedly summarize its application without new astounding information.

Though it has been successfully used in clinics for more than 10 years, two disadvantages of PET/CT still limit its use in clinics. First, unlike MR, CT cannot provide a high soft-tissue contrast and cannot precisely visualize the territories for some malignant lesions, such as tumors in the head and neck. Second, radiation exposure is a real concern for patients, especially for patients undergoing repeated PET/CT scans and pediatric patients, who are sensitive to ionizing radiation. It has been shown that a low-dose CT scan in PET/CT yields a radiation exposure of 2−3 mSv, while some CT protocols such as in CT perfusion imaging, because of repetitive imaging of the body region, can yield effective doses up to 20 mSv.[10] FDG-PET imaging usually causes effective dose levels on the order of 7−15 mSv, depending on the injected dose. Since a CT scan is required for both attenuation correction and anatomical correlation, it may provide an extra radiation burden. A recent study compared radiation in whole-body PET/CT examinations, PET scans after the administration of ^{18}F-FDG, and a fully diagnostic contrast-enhanced CT and revealed that up to 70% of the total exposure was contributed by CT.[49]

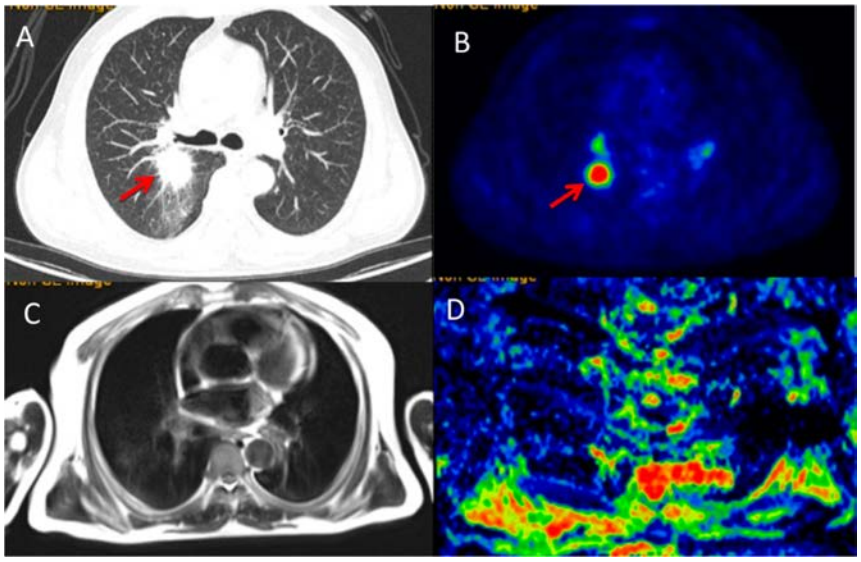

Figure 4. Images from a 62-year-old female with a non-small cell carcinoma lesion confirmed by pathology in the upper lobe of the right lung. Both the chest CT (A) and PET (B) clearly show the location and metabolism of the lesion (red arrow). However, it is not clearly shown at the same level by MRI (C) and DW-MRI (D) because of large artifacts.

3.2. Clinical Applications of PET/MRI. *3.2.1. Advantages of PET/MRI.* MRI, another imaging modality, can provide anatomical information. It is superior to CT in providing high-resolution anatomical information with excellent soft-tissue contrast, and it can also measure a variety of physiological, metabolic, and biochemical parameters that cannot be detected by CT.[50,51] Another major advantage of MRI compared with CT is that MRI is radiation-free, allowing patients to undergo multiple scans without concerns about radiation, especially in therapy monitoring and pediatric scanning. For these reasons, combining PET and MRI instead of PET and CT has become a topic of increasing interest in the imaging community over the past several years.

The combination of imaging modalities for high-sensitivity, high-resolution hybrid PET/MRI fusion imaging can be obtained in two different ways: one is to perform the PET and MRI scans individually in separate scanners and fuse the imaging with software, and the other is to scan the patient with an integrated PET/MRI system and obtain the PET and MRI images simultaneously. As a "one-stop shop", integrated PET/MRI can obtain anatomical, kinetic, functional, and metabolic information and other multiparametrics at the same time, and an integrated PET/MRI system can also simultaneously coregister various MRI and PET procedures. Theoretically, therefore, integrated PET/MRI is superior to separate PET and MRI scans. In 2007 BrainPET, the first integrated PET/MRI scanner for brain imaging, was developed by Schmand et al.,[52] who demonstrated for the first time that simultaneous PET and MRI data acquisition is feasible with integrated PET/MRI tomography, and the proof-of-principle simultaneous data acquisition was also confirmed by other groups.[41,53,54] A combined PET/MRI unit that may improve diagnostic accuracy by achieving an excellent spatial correlation between PET and MRI imaging therefore has a strong appeal to doctors. Studies exploring the clinical applications of PET/MRI for tumor imaging, neuron imaging, and cardiac imaging have been conducted in recent years.[55,72,85]

3.2.2. Applications of PET/MRI in Oncology. Since PET/CT is broadly used in tumor diagnostics, PET/MRI has also been studied in tumor diagnosis, staging, treatment response evaluation, and even to guide radiotherapy and surgical excision. Early diagnosis and distinguishing malignant from benign tumors is always a critical and core task for medical imaging. MRI provides high spatial resolution to define the tumor volume and localize the disease extent for tumor staging because of its superior soft-tissue contrast, and it is particularly useful for the evaluation of primary tumors that originate from anatomical sites that are suboptimally evaluated with CT. Therefore, PET/MRI is superior to PET/CT for some tumors, especially head and neck tumors, which are surrounded by abundant soft tissues. Drzezga et al.[55] first compared the diagnostic values of PET/CT and integrated PET/MR in oncology, where 32 various cancer patients underwent a single-injection, dual-imaging protocol consisting of a PET/CT scan and a subsequent PET/MRI scan. The results showed that there was no significant difference between the numbers of suspicious lesions or lesion-positive patients detected with PET/MRI and PET/CT, that anatomical allocation of PET/MRI was comparable to that of PET/CT, and that there was a high correlation between the mean SUVs measured with PET/MRI and PET/CT in the lesions. This revealed that PET/MRI is a reliable method comparable to PET/CT in detecting oncology. Boss et al.[56] prospectively showed that MRI provided excellent images without recognizable artifacts caused by the inserted PET system in eight patients with head and neck tumors by using simultaneous FDG PET/MRI after FDG PET/CT. They further showed that PET images from PET/MRI exhibited better spatial resolution and image contrast compared with those from PET/CT. Kuhn et al.[57] compared PET/CT and PET/MRI in 150 patients with head and neck cancer; their study indicated that PET/MRI yielded a higher diagnostic confidence for accurate lesion conspicuity, infiltration of adjacent structures, and perineural spread, indicating that PET/MRI can serve as a legitimate alternative to PET/CT in the clinical workup of patients with head and neck cancers.

Through the combination of anatomical MRI, diffusion-weighted MRI (DW-MRI), and PET imaging, some concerted information about cellularity and biological activity of the

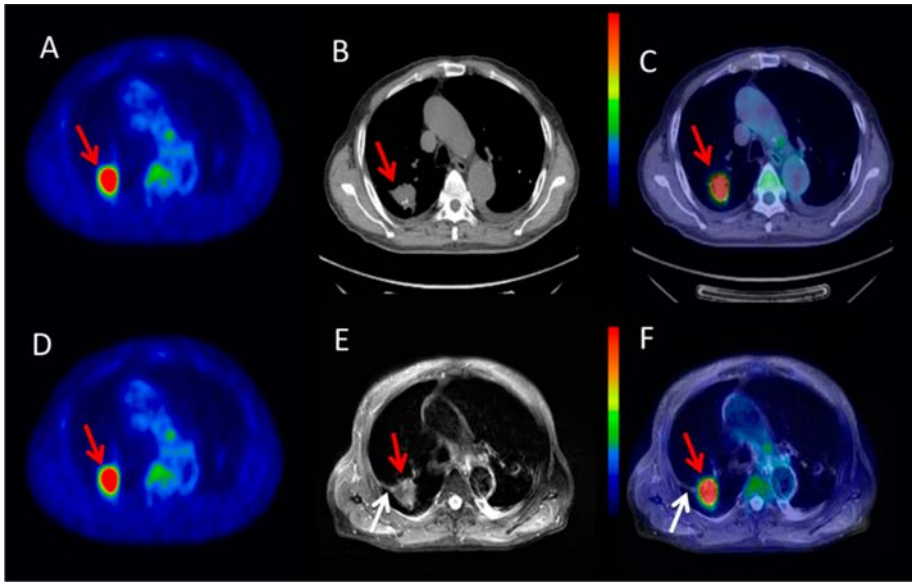

Figure 5. Images for a 58-year-old female with lung cancer confirmed by pathology. ^{18}F-FDG uptake was observed in PET images (A and D); both CT (B) and T_2-weighted MRI (T2MRI) (E) showed the main lesion (red arrow). However, only T2MRI (E) showed the pleural retraction accompanied by lung cancer (white arrow). PET/CT (C) showed only the main lesion, while PET/MR (F) showed both the main lesion and the pleural retraction.

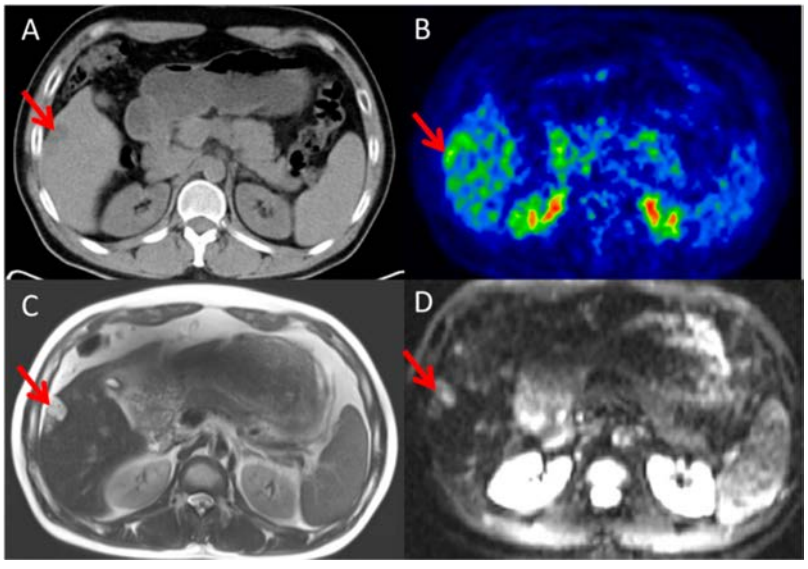

Figure 6. Images of a small hepatocellular carcinoma confirmed by pathology. CT (A) shows only slightly low density, and PET (B) also indicates a slightly higher metabolism than in normal tissue. However, it clearly appears in the corresponding T2MRI (C) and DW-MRI (D) images.

tumor could be obtained, and the assessment of tumor invasion into adjacent structures could probably be improved by the combination of anatomical MRI, DW-MRI, and PET in rectal, bladder, prostate, and gynecological cancers.[58,59] A recent study showed that the combination of MRI with ^{11}C-acetate PET/CT is superior to the individual methods alone in the detection of localized prostate cancer.[60] Furthermore, accuracy in the assessment of spreading to regional lymph nodes, especially in the pelvic region, the mediastinum, and the head and neck region, could also be improved.[61,62] Therefore, it is anticipated that the sensitivity and specificity in oncology staging can be improved.

PET/MRI is a new technology with lower radiation levels compared with PET/CT. Although it has similar diagnostic performance in tumor detection compared with PET/CT,[63] it still could not replace PET/CT completely. Most of the time, the information provided by PET/CT and PET/MRI can be complementary with each other because the two methods are based on completely different biophysical and biochemical underpinnings. Since the structure of tissues is different, the detection accuracy for tumors in different parts of the body may not be the same for CT and MRI. In the thorax, where the density of protons is lower and the artifacts originate from respiration or the gas−tissue boundary, which can significantly decrease the sensitivity of MRI, echo planar imaging (EPI)-based MRI is susceptible to image distortions. Thus, because of those limitations, small lesions in the thorax are always ignored by MRI (Figure 4). MRI provides high soft-tissue contrast and it may more easily visualize the diffusion of the tumor compared with CT. For example, pleural retraction of lung

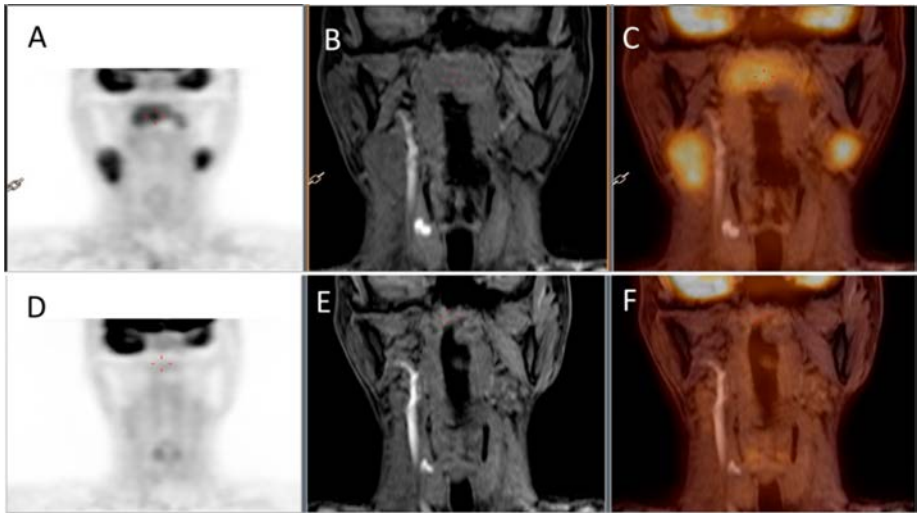

Figure 7. Images for a 52-year-old male with nasopharyngeal carcinoma confirmed by pathology with bilateral neck lymph node metastasis. It can be detected by PET (A), MRI (B), and PET/MRI before therapy. After two months of therapy, ^{18}F-FDG uptake was significantly decreased in PET (D) and PET/MRI (F), while the nasopharyngeal lesion and neck lymph node was also significantly reduced when detected by MRI (E).

cancer can be clearly detected by MRI (Figure 5). Recently, Rauscher et al.[64] systemically compared PET/MRI with PET/CT in the characterization of chest and abdominal lesions. They concluded that overall the PET image quality and detection rate of ^{18}F-FDG-positive lung lesions in PET/MRI is equivalent to that in PET/CT but that the detection rate of small lung lesions by PET/MR is lower than that by PET/CT. On the contrary, the sensitivity of PET/MRI is superior to that of PET/CT in detecting tumors inside the abdominal cavity. For example, it is well-known that the uptake of ^{18}F-FDG in hepatocellular carcinoma and kidney malignancy is very small and difficult to visualize by PET/CT, yet MRI is sensitive enough to detect such small lesions in the liver (Figure 6) or kidney.

Accurate assessment of the tumor response is essential in clinical patient management as well as in drug development. Currently, the response is mainly evaluated by anatomical measures based on standardized criteria for response evaluation in solid tumors by PET/CT (PERCIST), which was suggested in 2009 in parallel with the increasing amount of evidence on FDG-PET as a surrogate marker for the response. Similar results have emerged for DW-MRI from a broad range of cancer types,[65,66] suggesting that early changes in tumor diffusion values are correlated with the response to therapy and indicating that PET/MRI could be an effective and valuable method in early therapy evaluation (Figure 7). However, by reviewing 900 patients who underwent cancer assessments with PET/MRI, Czernin et al.[67] surprisingly found that PET/MRI did not show a striking difference in diagnostic accuracy for cancer assessment. Thus, the controversy over the value of PET/MRI in tumor assessment still exists, and to uncover the truth, a multicenter study with a large number of patients may be necessary.

DW-MRI measures cell density and is based on diffusion of water molecules in tissues. MR spectroscopy (MRS) can be used to monitor metabolic processes and products. Advanced functional MRI techniques such as DW-MRI, MRS, and perfusion-weighted imaging used with PET can further enhance the detection and characterization of malignant lesions for prognosis assessment, biopsy and pretreatment planning, patient selection for certain therapeutic agents, and response prediction and assessment.[68,69]

3.2.3. Applications of PET/MRI in Neurological Disease. PET/MRI can provide an integrated multidimensional and multiparametric structural and functional assessment of the central nervous system in patients with neurodegenerative, ischemic, and neurological diseases and improve the accurate diagnosis of those diseases. It is also valuable in evaluating biological processes such as metabolism, perfusion, oxygen consumption, receptor expression, and function even in the smallest neurological−anatomical structures.[70,71] The high degrees of spatial and temporal coregistration of PET and MRI data sets are particularly feasible in neurological oncology, in which accurate alignment of structural and functional information is essential for biopsy and treatment planning.

Garibotto et al.[72] successfully scanned 15 patients with neurodegenerative disease, epilepsy, or high-grade tumors using PET/MRI. Their clinical study showed that acquiring both PET and MRI data in a single session with a hybrid system could minimize patient discomfort while maximizing clinical information and optimizing registration of both modalities. Hitz et al.[73] compared integrated whole-body PET/MR imaging with conventional PET/CT in 30 suspected dementia patients. The results showed that lower measured PET signal values were obtained throughout the brain in region of interest (ROI)-based quantification of the PET signal for PET/MRI compared with PET/CT. It was inferred that PET/MRI is a valuable tool in detecting neurodegenerative disease.

The brain is an organ with abundant receptors that play critical roles in brain function, and the abnormal expression of various receptors is the main reason for different neurological diseases such as Parkinson's disease, Alzheimer's disease, and so on. Imaging of the expression of receptors and detecting their function are valuable in diagnosis and treatment planning for many brain diseases. Son et al.[74] measured the activity of individual raphe nuclei with fluorine ^{18}F-FDG and ^{11}C-DASB imaging with PET/MRI. Each raphe nucleus could be distinguished in both FDG and ^{11}C-DASB images. The standard uptake value ratio of FDG and the nondisplaceable binding potential of ^{11}C-DASB were significantly correlated. In this study, the serotonergic activity, including both glucose

dx.doi.org/10.1021/mp500321h | *Mol. Pharmaceutics* 2014, 11, 3798−3809

metabolism and the transporter-binding potential of the raphe nuclei, was successfully measured by a brain-dedicated PET/MRI system. By detecting the expression of the somatostatin receptor in meningioma, Thorwarth et al.[75] first guided intensity-modulated radiotherapy (IMRT) treatment planning in patients with meningioma via integrated PET/MRI with ^{68}Ga-DOTATOC as the biomarker. Target volumes for IMRT treatment planning did not differ between MRI plus ^{68}Ga-DOTATOC PET/CT and simultaneous PET/MR imaging, and thus, the overall volume of the PET/MRI-based planning target volumes (PTVs) was approximately the same as that obtained from PET/CT. However, a small region of infiltrative tumor growth next to the main tumor mass was better visualized with combined PET/MRI, and therefore, an IMRT treatment plan was optimized for the PTV by PET/MRI.

The combination of MRI and PET will provide more information for brain tumors and may be an alternative method for brain tumor grading. In Dunvet's study, 38 glioma patients underwent conventional MRI, MRS, diffusion sequences, and fluoroethyltyrosine PET (FET-PET).[76] The tumor time−activity curve reached the best accuracy by distinguishing between low- and high-grade gliomas followed by ADC histogram analysis. Combining the time−activity curve and ADC histogram analyses improved the sensitivity from 67% to 86% and the specificity from 63−67% to 100%. This study indicated that FET-PET/MRI may be valuable in the initial assessment of the primary brain.

Surgical resection is an important method in treating some neurological diseases by precisely removing the lesion without destroying the normal tissue, which is critical for the prognosis. PET/MRI is not only useful in diagnosis but also valuable in guiding surgical removal. Combining MRI and PET information increases the sensitivity of the presurgical evaluation for medically refractory epilepsy by FDG-PET/MRI, which has been successfully performed at the University of California, Los Angeles.[77] Recently, a multimodality imaging approach using FDG-PET/MRI coregistration and diffusion tensor imaging has been demonstrated to be useful in presurgical evaluation to localize epileptogenic tubers.[78]

3.2.4. Applications of PET/MRI in Cardiology. In the clinical assessment of patients with cardiovascular disease, PET allows the quantification of blood flow and is considered the gold standard for assessing myocardial tissue viability. MRI can provide information about ventricle function and structural changes, and by the use of contrast agents, perfusion and tissue viability can be detected. It was suggested that the combination of these methods in a simultaneous PET/MRI scanner would allow a more detailed at-risk assessment of the myocardium.

In cardiology, PET imaging is still most frequently used for the diagnosis of obstructive coronary artery disease (CAD). It provides the most accurate noninvasive means of diagnosing obstructive CAD, with a sensitivity and specificity of about 90%,[79−81] and has been proven to be valuable for accurate prognosis and good patient management.[82−84] MRI also has great promise in the diagnosis of obstructive CAD, where coronary artery stenosis can be detected by first-pass MRI after injection of a fast bolus of a gadolinium contrast agent such as gadolinium−diethylenetriaminepentaacetic acid (DTPA), yielding a sensitivity and specificity of about 91% and 81%, respectively.[85,86]

Ischemic myocardium that is dysfunctional but viable has the potential for recovery of contractile function after revascularization.^{18}F-FDG PET is considered to be the gold standard among the different imaging modalities in assessing myocardial viability.[87,88] The results of several studies have proven the value of ^{18}F-FDG PET imaging in identifying those patients on the basis of a prediction of improved left ventricle function.[89,90] Contrast-enhanced MRI appears to be a promising alternative that is capable of visualizing the transmural distribution of viable and infarcted myocardium with excellent spatial resolution.[91] A comparison of delayed-enhancement MRI with ^{18}F-FDG PET and $^{13}NH_3$ in 31 patients with ischemic heart failure revealed that the location and extent of infarct scarring, as delineated by delayed enhancement, correlated very well with the nonviable segments from PET.[92] Besides the detection of the perfusion and viability of the myocardium, PET/MRI can also be used in other aspects of myocardial disease. With a new radiotracer, PET/MRI can also image angiogenesis that occurs in response to ischemia and inflammation that is a part of the healing process after ischemic tissue injury. ^{18}F-galacto-RGD PET can image the expression of integrin in response to myocardial infarction, and the delayed enhancement of the MRI signal allows exact localization of ^{18}F-galacto-RGD uptake in the region of the myocardial infarction.[93] Stem cell transplantation and gene therapy is a promising treatment for cardiac disease, and therefore, monitoring of the transplanted stem cell and the expressed gene is valuable in predicting the prognosis. Thus, PET/MRI should be feasible for visualization of the survival of stem cells and localization of reporter gene expression.

4. SUMMARY

Almost seven years have passed since the debut of integrated PET/MRI, but PET/MRI is still in its early stages of development. Although MRI is superior to CT in several respects, PET/MRI still faces some challenging technique problems, such as cost and time consumption, which are disadvantages that limit its use in clinical settings. At present, PET/CT is still a popular and valuable tool in clinics, so it should not be replaced by PET/MRI. However, we anticipate that with the development of PET/MRI and the installation of more PET/MRI scanners, imaging of disease with PET/MRI will become widespread and patients will benefit from the promotion of new hybrid PET technologies.

■ AUTHOR INFORMATION

Corresponding Authors

*J.W.: Address: 127# West Changle Road, 710032 Xi'an, China. E-mail: wangjing@fmmu.edu.cn.

*J.T.: Address: 95 Zhongguancun East Road, 100190 Beijing, China. Tel: +86 10 82618465. Fax: +86 10 62527995. E-mail: tian@ieee.org.

Author Contributions

§Z.H., W.Y., H.L., and K.W. contributed equally.

Notes

The authors declare no competing financial interest.

■ ACKNOWLEDGMENTS

This work was supported by the National Basic Research Program of China (973 Program) (Grant 2011CB707700), the National Natural Science Foundation of China (Grants 81227901, 61231004, 61302024, 81371594, and 81230033), the National Key Technology R&D Program (Grants 2012BAI23B01 and 2012BAI23B06), the Chinese Academy of Sciences Visiting Professorship for Senior International

Scientists (Grant 2013T1G0013), and the Fellowship for Young International Scientists of the Chinese Academy of Sciences (Grants 2013Y1GB0005 and 2013Y1GA0004). We thank Yawei Qu and Xiaojun Zhang for technical assistance in conducting this research.

■ ABBREVIATIONS

PET, positron emission tomography; MRI, magnetic resonance imaging; SPECT, single-photon-emission computed tomography; PMT, photomultiplier tube; CT, computed tomography; BGO, bismuth germanium oxide; GSO, gadolinium oxyorthosilicate; LSO, lutetium oxyorthosilicate; TOF, time of flight; SNR, signal-to-noise ratio; APD, avalanche photodiode; SiPM, silicon photomultiplier; RF, radiofrequency; FOV, field of view; DOI, depth of interaction; UTE, ultrashort echo time; MLAA, maximum-likelihood reconstruction of attenuation and activity; EPI, echo planar imaging; CAD, coronary artery disease; DTPA, diethylenetriaminepentaacetic acid.

■ REFERENCES

(1) Phelps, M. E. The merging of biology and imaging into molecular imaging. *J. Nucl. Med.* **2000**, *41*, 661−681.
(2) Ruth, T. Accelerating production of medical isotopes. *Nature* **2009**, *457*, 536−537.
(3) Miller, G. Alzheimer's biomarker initiative hits its stride. *Science* **2009**, *326*, 386−389.
(4) Friston, K. J. Modalities, modes, and models in functional neuroimaging. *Science* **2009**, *326*, 399−403.
(5) Bar-Shalom, R.; Valdivia, A. Y.; Blaufox, M. D. PET imaging in oncology. *Semin. Nucl. Med.* **2000**, *30*, 150−185.
(6) Schwaiger, M.; Ziegler, S.; Nekolla, S. G. PET/CT: Challenge for nuclear cardiology. *J. Nucl. Med.* **2005**, *46*, 8a−9a.
(7) Beyer, T.; Townsend, D. W.; Brun, T.; Kinahan, P. E.; Charron, M.; Roddy, R.; Jerin, J.; Young, J.; Byars, L.; Nutt, R. A combined PET/CT scanner for clinical oncology. *J. Nucl. Med.* **2000**, *41*, 1369−1379.
(8) Jolles, P. R.; Chapman, P. R.; Alavi, A. PET, CT and MRI in the evaluation of neuropsychiatric disorder: Current applications. *J. Nucl. Med.* **1989**, *30*, 1589−1606.
(9) Donadieu, J.; Roudier, C.; Saguintaah, M.; Maccia, C.; Chiron, R. Estimation of the radiation dose from CT in cystic fibrosis. *Chest* **2007**, *132*, 1233−1238.
(10) Brix, G.; Lechel, U.; Glatting, G.; Ziegler, S. I.; Münzing, W.; Müller, S. P.; Beyer, T. Radiation exposure of patients undergoing whole-body dual-modality ^{18}F-FDG PET/CT examinations. *J. Nucl. Med.* **2005**, *46*, 608−613.
(11) Cannon, W. B. The movements of the intestines studied by means of the Röntgen rays. *J. Med. Res.* **1902**, *7*, 72−75.
(12) Tselos, G. D. New Jersey's Thomas Edison and the fluoroscope. *N. J. Med.* **1995**, *92*, 731−733.
(13) Becquerel, J.; Crowther, J. A. Discovery of radioactivity. *Nature* **1948**, *161*, 609.
(14) Jadvar, H.; Colletti, P. M. Competitive advantage of PET/MRI. *Eur. J. Radiol.* **2014**, *83*, 84−94.
(15) Delso, G.; Ziegler, S. PET/MR system design. In *PET/MRI*; Springer: Berlin, 2014; pp 1−19.
(16) Herzog, H.; Pietrzyk, U.; Shah, N. J.; Ziemons, K. The current state, challenges and perspectives of MR-PET. *Neuroimage* **2010**, *49*, 2072−2082.
(17) Sauter, A. W.; Wehrl, H. F.; Kolb, A.; Judenhofer, M. S.; Pichler, B. J. Combined PET/MRI: One step further in multimodality imaging. *Trends Mol. Med.* **2010**, *16*, 508−515.
(18) Bezrukov, I.; Mantlik, F.; Schmidt, H.; Schölkopf, B.; Pichler, B. J. MR-Based PET attenuation correction for PET/MR imaging. *Semin. Nucl. Med.* **2013**, *43*, 45−59.
(19) Andersen, F. L.; Ladefoged, C. N.; Beyer, T.; Keller, S. H.; Hansen, A. E.; Højgaard, L.; Kjær, A.; Law, I.; Holm, S. Combined PET/MR imaging in neurology: MR-based attenuation correction implies a strong spatial bias when ignoring bone. *Neuroimage* **2014**, *84*, 206−216.
(20) Kalemis, A.; Delattre, B. M.; Heinzer, S. Sequential whole-body PET/MR scanner: Concept, clinical use, and optimization after two years in the clinic. The manufacturer's perspective. *MAGMA* **2013**, *26*, 5−23.
(21) Zaidi, H.; Ojha, N.; Morich, M.; Griesmer, J.; Hu, Z.; Maniawski, P.; Ratib, O.; Izquierdo-Garcia, D.; Fayad, Z. A.; Shao, L. Design and performance evaluation of a whole-body Ingenuity TF PET/MRI system. *Phys. Med. Biol.* **2011**, *56*, 3091−3106.
(22) Veit-Haibach, P.; Kuhn, F. P.; Wiesinger, F.; Delso, G.; von Schulthess, G. PET-MR imaging using a tri-modality PET/CT-MR system with a dedicated shuttle in clinical routine. *MAGMA* **2013**, *26*, 25−35.
(23) Queiroz, M. A.; Hüllner, M.; Kuhn, F.; Huber, G.; Meerwein, C.; Kollias, S.; von Schulthess, G.; Veit-Haibach, P. PET/MRI and PET/CT in follow-up of head and neck cancer patients. *Eur. J. Nucl. Med. Mol. Imaging* **2014**, *41*, 1066−1075.
(24) Peng, B. J.; Wu, Y.; Cherry, S. R.; Walton, J. H. New shielding configurations for a simultaneous PET/MRI scanner at 7 T. *J. Magn. Reson.* **2014**, *239*, 50−56.
(25) Gilbert, K. M.; Scholl, T. J.; Handler, W. B.; Alford, J. K.; Chronik, B. A. Evaluation of a positron emission tomography (PET)-compatible field-cycled MRI (FCMRI) scanner. *Magn. Reson. Med.* **2009**, *62*, 1017−1025.
(26) Mackewn, J. E.; Strul, D.; Hallett, W. A.; Halsted, P.; Page, R. A.; Keevil, S. F.; Williams, S. C. R.; Cherry, S. R.; Marsden, P. K. Design and development of an MR-compatible PET scanner for imaging small animals. *IEEE Trans. Nucl. Sci.* **2005**, *52*, 1376−1380.
(27) Poole, M.; Bowtell, R.; Green, D.; Pittard, S.; Lucas, A.; Hawkes, R.; Carpenter, A. Split gradient coils for simultaneous PET/MRI. *Magn. Reson. Med.* **2009**, *62*, 1106−1111.
(28) Yamamoto, S.; Hatazawa, J.; Imaizumi, M.; Shimosegawa, E.; Aoki, M.; Sugiyama, E.; Kawakami, M.; Takamatsu, S.; Minato, K.; Matsumoto, K.; Senda, M. A multi-slice dual layer MR-compatible animal PET system. *IEEE Trans. Nucl. Sci.* **2009**, *56*, 2706−2713.
(29) Lucas, A. J.; Hawkes, R. C.; Ansorge, R. E.; Williams, G. B.; Nutt, R. E.; Clark, J. C.; Fryer, T. D.; Carpenter, T. A. Development of a combined microPET-MR system. *Technol. Cancer Res. Treat.* **2006**, *5*, 337−341.
(30) Spanoudaki, V. C.; Mann, A. B.; Otte, A. N.; Konorov, I.; Torres-Espallardo, I.; Paul, S.; Ziegler, S. I. Use of single photon counting detector arrays in combined PET/MR: Characterization of LYSO-SiPM detector modules and comparison with a LSO-APD detector. *J. Instrum.* **2007**, *2*, No. P12002.
(31) Delso, G.; Fürst, S.; Jakoby, B.; Ladebeck, R.; Ganter, C.; Nekolla, S. G.; Schwaiger, M.; Ziegler, S. I. Performance measurements of the Siemens mMR integrated whole-body PET/MR scanner. *J. Nucl. Med.* **2011**, *52*, 1914−1922.
(32) Torigian, D. A.; Zaidi, H.; Kwee, T. C.; Saboury, B.; Udupa, J. K.; Cho, Z. H.; Alavi, A. PET/MR imaging: Technical aspects and potential clinical applications. *Radiology* **2013**, *267*, 26−44.
(33) Wetter, A.; Lipponer, C.; Nensa, F.; Heusch, P.; Rübben, H.; Altenbernd, J.; Schlosser, T.; Bockisch, A.; Pöppel, T.; Lauenstein, T.; Nagarajah, J. Evaluation of the PET component of simultaneous [^{18}F]choline PET/MRI in prostate cancer: Comparison with [^{18}F]-choline PET/CT. *Eur. J. Nucl. Med. Mol. Imaging* **2014**, *41*, 79−88.
(34) Pace, L.; Nicolai, E.; Luongo, A.; Aiello, M.; Catalano, O. A.; Soricelli, A.; Salvatore, M. Comparison of whole-body PET/CT and PET/MRI in breast cancer patients: Lesion detection and quantitation of ^{18}F-deoxyglucose uptake in lesions and in normal organ tissues. *Eur. J. Radiol.* **2014**, *83*, 289−296.
(35) Wiesmüller, M.; Quick, H. H.; Navalpakkam, B.; Lell, M. M.; Uder, M.; Ritt, P.; Schmidt, D.; Beck, M.; Kuwert, T.; von Gall, C. C. Comparison of lesion detection and quantitation of tracer uptake between PET from a simultaneously acquiring whole-body PET/MR hybrid scanner and PET from PET/CT. *Eur. J. Nucl. Med. Mol. Imaging* **2013**, *40*, 12−21.

(36) Tu, C.; Ng, T. S.; Jacobs, R. E.; Louie, A. Y. Multimodality PET/MRI agents targeted to activated macrophages. *J. Biol. Inorg. Chem.* **2014**, *19*, 247−258.
(37) Mansi, L.; Ciarmiello, A. Perspectives on PET/MR Imaging: Are we ready for clinical use? *J. Nucl. Med.* **2014**, DOI: 10.2967/jnumed.113.133405.
(38) Keereman, V.; Mollet, P.; Berker, Y.; Schulz, V.; Vandenberghe, S. Challenges and current methods for attenuation correction in PET/MR. *MAGMA* **2013**, *26*, 81−98.
(39) Hofmann, M.; Steinke, F.; Scheel, V. MRI-based attenuation correction for PET/MRI: A novel approach combining pattern recognition and atlas registration. *J. Nucl. Med.* **2008**, *49*, 1875−1883.
(40) Martinez-Möller, A.; Souvatzoglou, M.; Delso, G.; Bundschuh, R. A.; Chefd'hotel, C.; Ziegler, S. I.; Navab, N.; Schwaiger, M.; Nekolla, S. G. Tissue classification as a potential approach for attenuation correction in whole-body PET/MRI: Evaluation with PET/CT data. *J. Nucl. Med.* **2009**, *50*, 520−526.
(41) Catana, C.; van der Kouwe, A.; Benner, T. Toward implementing an MRI-based PET attenuation-correction method for neurologic studies on the MR-PET brain prototype. *J. Nucl. Med.* **2010**, *51*, 1431−1438.
(42) Keereman, V.; D'Asseler, Y.; Van Holen, R.; Mollet, P.; Vandenberghe, S. The effect of interpatient attenuation coefficient variability on segmented attenuation correction for PET. *J. Nucl. Med.* **2010**, *51*, 1378.
(43) Schramm, G.; Langner, J.; Hofheinz, F.; Petr, J.; Beuthien-Baumann, B.; Platzek, I.; Steinbach, J.; Kotzerke, J.; van den Hoff, J. Quantitative accuracy of attenuation correction in the Philips Ingenuity TF whole-body PET/MR system: A direct comparison with transmission-based attenuation correction. *MAGMA* **2013**, *26*, 115−126.
(44) Mollet, P.; Keereman, V.; Bini, J.; Izquierdo-Garcia, D.; Fayad, Z. A.; Vandenberghe, S. Improvement of attenuation correction in time-of-flight PET/MR imaging with a positron-emitting source. *J. Nucl. Med.* **2014**, *55*, 329−336.
(45) Nuyts, J.; Dupont, P.; Stroobants, S.; Benninck, R.; Mortelmans, L.; Suetens, P. Simultaneous maximum a posteriori reconstruction of attenuation and activity distributions from emission sinograms. *IEEE Trans. Med. Imaging* **1999**, *18*, 393−403.
(46) Nuyts, J.; Bal, G.; Kehren, F.; Fenchel, M.; Michel, C.; Watson, C. Completion of a truncated attenuation image from the attenuated PET emission data. *IEEE Trans. Med. Imaging* **2013**, *32*, 237−246.
(47) Defrise, M.; Rezaei, A.; Nuyts, J. Time-of-flight PET data determine the attenuation sinogram up to a constant. *Phys. Med. Biol.* **2012**, *57*, 885−899.
(48) Boellaard, R.; Hofman, M. B.; Hoekstra, O. S.; Lammertsma, A. A. Accurate PET/MR quantification using time of flight MLAA image reconstruction. *Mol. Imaging Biol.* **2014**, *16*, 469−477.
(49) Brix, G.; Beyer, T. PET/CT: Dose-escalated image fusion? *Nuklearmedizin* **2005**, *44*, 51−57.
(50) Goldberg, M. F.; Chawla, S.; Alavi, A.; Torigian, D. A.; Melhem, E. R. PET and MRI of brain tumors. *PET Clin.* **2008**, *3*, 293−315.
(51) Antoch, G.; Bockisch, A. Combined PET/MRI: A new dimension in whole-body oncology imaging? *Eur. J. Nucl. Med. Mol. Imaging* **2009**, *36* (Issue 1 Suppl.), 113−120.
(52) Schmand, M.; Burbar, Z.; Corbeil, J.; Zhang, N.; Michael, C.; Byars, L.; Eriksson, L.; Grazioso, R.; Martin, M.; Moor, A.; Camp, J.; Matschl, V.; Ladebeck, R.; Renz, W.; Fischer, H.; Jattke, K.; Schnur, G.; Rietsch, N.; Bendriem, B.; Heiss, W. BrainPET: First human tomograph for simultaneous (functional) PET and MR imaging. *J. Nucl. Med.* **2007**, *48* (Suppl. 2), 45P.
(53) Schlemmer, H. P.; Pichler, B. J.; Schmand, M.; Burbar, Z.; Michael, C.; Ladebeck, R.; Jattke, K.; Townsend, D.; Nahmias, C.; Jacob, P. K.; Heiss, W. D.; Claussen, C. D. Simultaneous MR/PET imaging of the human brain: Feasibility study. *Radiology* **2008**, *248*, 1028−1035.
(54) Herzog, H.; Langen, K. J.; Weirich, C.; Rota Kops, E.; Kaffanke, J.; Tellmann, L.; Scheins, J.; Neuner, I.; Stoffels, G.; Fischer, K.; Caldeira, L.; Coenen, H. H.; Shah, N. J. High resolution BrainPET combined with simultaneous MRI. *Nuklearmedizin* **2011**, *50*, 74−82.
(55) Drzezga, A.; Souvatzoglou, M.; Eiber, M.; Beer, A. J.; Furst, S.; Martinez-Möller, A.; Nekolla, S. G.; Ziegler, S.; Ganter, C.; Rummeny, E. J.; Schwaiger, M. First clinical experience with integrated whole-body PET/MR: Comparison to PET/CT in patients with oncologic diagnoses. *J. Nucl. Med.* **2012**, *53*, 845−855.
(56) Boss, A.; Stegger, L.; Bisdas, S.; Kolb, A.; Schwenzer, N.; Pfister, M.; Claussen, C. D.; Pichler, B. J.; Pfannenberg, C. Feasibility of simultaneous PET/MR imaging in the head and upper neck area. *Eur. Radiol.* **2011**, *21*, 1439−1446.
(57) Kuhn, F. P.; Hüllner, M.; Mader, C. E.; Kastrinidis, N.; Huber, G. F.; von Schulthess, G. K.; Kollias, S.; Veit-Haibach, P. Contrast-enhanced PET/MR imaging versus contrast-enhanced PET/CT in head and neck cancer: How much MR information is needed? *J. Nucl. Med.* **2014**, *55*, 551−558.
(58) Punwani, S. Diffusion weighted imaging of female pelvis cancers: Concepts and clinical applications. *Eur. J. Radiol.* **2011**, *78*, 21−29.
(59) Giannarini, G.; Petralia, G.; Thoeney, H. C. Potential and limitations of diffusion-weighted magnetic resonance imaging in kidney, prostate, and bladder cancer including pelvic lymph node staging: A critical analysis of the literature. *Eur. Urol.* **2012**, *61*, 326−340.
(60) Jambor, I.; Borra, R.; Kemppainen, J. Improved detection of localized prostate cancer using co-registered MRI and ^{11}C-acetate PET/CT. *Eur. J. Radiol.* **2012**, *81*, 2966−2972.
(61) Hochhegger, B.; Marchiori, E.; Sedlaczek, O.; Irion, K.; Heussel, C. P.; Ley, S.; Ley-Zaporozhan, J.; Soares Souza, A., Jr.; Kauczor, H. U. MRI in lung cancer: A pictorial essay. *Br. J. Radiol.* **2011**, *84*, 661−668.
(62) Jansen, J. F. A.; Schöder, H.; Lee, N. Y.; Stambuk, H. E.; Wang, Y.; Fury, M. G.; Patel, S. G.; Pfister, D. G.; Shah, J. P.; Koutcher, J. A.; Shukla-Dave, A. Tumor metabolism and perfusion in head and neck squamous cell carcinoma: Pretreatment multimodality imaging with ^{1}H magnetic resonance spectroscopy, dynamic contrast-enhanced MRI and [^{18}F]FDG-PET. *Int. J. Radiat. Oncol. Biol. Phys.* **2012**, *82*, 299−307.
(63) Tian, J.; Fu, L.; Yin, D.; Zhang, J.; Chen, Y.; An, N.; Xu, B. Does the novel integrated PET/MRI offer the same diagnostic performance as PET/CT for oncological indications? *PLoS One* **2014**, *9*, No. e90844.
(64) Rauscher, I.; Eiber, M.; Fürst, S.; Souvatzoglou, M.; Nekolla, S.; Ziegler, S.; Rummeny, E.; Schwaiger, M.; Beer, A. PET/MR imaging in the detection and characterization of pulmonary lesions: Technical and diagnostic evaluation in comparison to PET/CT. *J. Nucl. Med.* **2014**, *55*, 724−729.
(65) Galbán, S.; Brisset, J. C.; Rehemtulla, A.; Chenevert, T. L.; Ross, B. D.; Galbán, C. J. Diffusion-weighted MRI for assessment of early cancer treatment response. *Curr. Pharm. Biotechnol.* **2010**, *11*, 701−708.
(66) Heijmen, L.; Verstappen, M. C.; TerVoert, E. E.; Punt, C. J.; Oyen, W. J.; deGeus-Oei, L. F.; Hermans, J. J.; Heerschap, A.; van Laarhoven, H. W. Tumour response prediction by diffusion-weighted MR imaging: Ready for clinical use? *Crit. Rev. Oncol. Hematol.* **2012**, *83*, 194−207.
(67) Czernin, J.; Ta, L.; Herrmann, K. Does PET/MR imaging improve cancer assessments? Literature evidence from more than 900 patients. *J. Nucl. Med.* **2014**, *55*, 59S−62S.
(68) Kwee, T. C.; Takahara, T.; Ochiai, R. Whole-body diffusion-weighted magnetic resonance imaging. *Eur. J. Radiol.* **2009**, *70*, 409−417.
(69) Low, R. N.; Gurney, J. Diffusion-weighted MRI (DWI) in the oncology patient: Value of breath hold DWI compared to unenhanced and gadolinium-enhanced MRI. *J. Magn. Reson. Imaging* **2007**, *25*, 848−858.
(70) Boss, A.; Bisdas, S.; Kolb, A. Hybrid PET/MRI of intracranial masses: Initial experiences and comparison to PET/CT. *J. Nucl. Med.* **2010**, *51*, 1198−1205.

(71) Cho, Z. H.; Son, Y. D.; Kim, H. K. Substructural hippocampal glucose metabolism observed on PET/MRI. *J. Nucl. Med.* **2010**, *51*, 1545−1548.
(72) Garibotto, V.; Heinzer, S.; Vulliemoz, S.; Guignard, R.; Wissmeyer, M.; Seeck, M.; Lovblad, K. O.; Zaidi, H.; Ratib, O.; Vargas, M. I. Clinical applications of hybrid PET/MRI in neuroimaging. *Clin. Nucl. Med.* **2013**, *38*, e13−e18.
(73) Hitz, S.; Habekost, C.; Fürst, S.; Delso, G.; Förster, S.; Ziegler, S.; Nekolla, S. G.; Souvatzoglou, M.; Beer, A. J.; Grimmer, T.; Eiber, M.; Schwaiger, M.; Drzezga, A. Systematic comparison of the performance of integrated whole-body PET/MR imaging to conventional PET/CT for ^{18}F-FDG brain imaging in patients examined for suspected dementia. *J. Nucl. Med.* **2014**, *55*, 923−931.
(74) Son, Y. D.; Cho, Z. H.; Choi, E. J.; Kim, J. H.; Kim, H. K.; Lee, S. Y.; Chi, J. G.; Park, C. W.; Kim, J. H.; Kim, Y. B. Individually differentiated serotonergic raphe nuclei measured with brain PET/MR imaging. *Radiology* **2014**, DOI: http://dx.doi.org/10.1148/radiol.14131547.
(75) Thorwarth, D.; Müller, A. C.; Pfannenberg, C.; Beyer, T. Combined PET/MR imaging using ^{68}Ga-DOTATOC for radiotherapy treatment planning in meningioma patients. *Recent Results Cancer Res.* **2013**, *194*, 425−439.
(76) Dunet, V.; Maeder, P.; Nicod-Lalonde, M.; Lhermitte, B.; Pollo, C.; Bloch, J.; Stupp, R.; Meuli, R.; Prior, J. O. Combination of MRI and dynamic FET PET for initial glioma grading. *Nuklearmedizin* **2014**, DOI: 10.3413/Nukmed-0650-14-03.
(77) Lee, K. K.; Salamon, N. [^{18}F]Fluorodeoxyglucose−positron-emission tomography and MR imaging coregistration for presurgical evaluation of medically refractory epilepsy. *Am. J. Neuroradiol.* **2009**, *30*, 1811−1816.
(78) Chandra, P. S.; Salamon, N.; Huang, J. FDG-PET/MRI coregistration and diffusion-tensor imaging distinguish epileptogenic tubers and cortex in patients with tuberous sclerosis complex: A preliminary report. *Epilepsia* **2006**, *47*, 1543−1549.
(79) Nekolla, S. G.; Martinez-Möller, A.; Saraste, A. PET and MRI in cardiac imaging: From validation studies to integrated applications. *Eur. J. Nucl. Med. Mol. Imaging* **2009**, *36*, S121−S130.
(80) Klocke, F. J.; Baird, M. G.; Lorell, B. H.; Bateman, T. M.; Messer, J. V.; O'Gara, P. T.; Carabello, B. A.; Russell, R. O.; Cerqueira, M. D., Jr.; St John Sutton, M. G.; DeMaria, A. N.; Udelson, J. E.; Kennedy, J. W.; Verani, M. S.; Williams, K. A.; Antman, E. M.; Smith, S. C.; Alpert, J. S., Jr.; Gregoratos, G.; Anderson, J. L.; Hiratzka, L. F.; Faxon, D. P.; Hunt, S. A.; Fuster, V.; Jacobs, A. K.; Gibbons, R. J.; Russell, R. O. American College of Cardiology; American Heart Association Task Force on Practice Guidelines; American Society for Nuclear Cardiology. ACC/AHA/ASNC guidelines for the clinical use of cardiac radionuclide imaging—Executive summary: A report of the American College of Cardiology/American Heart Association Task Force on Practice Guidelines (ACC/AHA/ ASNC Committee To Revise the 1995 Guidelines for the Clinical Use of Cardiac Radionuclide Imaging). *J. Am. Coll. Cardiol.* **2003**, *42*, 1318−1333.
(81) Parker, M. W.; Iskandar, A.; Limone, B. Diagnostic accuracy of cardiac positron emission tomography versus single photon emission computed tomography for coronary artery disease: A bivariate meta-analysis. *Circ. Cardiovasc. Imaging* **2012**, *5*, 700−707.
(82) McArdle, B. A.; Dowsley, T. F.; deKemp, R. A.; Wells, G. A.; Beanlands, R. S. Does rubidium-82 PET have superior accuracy to SPECT perfusion imaging for the diagnosis of obstructive coronary disease? A systematic review and meta-analysis. *J. Am. Coll. Cardiol.* **2012**, *60*, 1828−1837.
(83) Fukushima, K.; Javadi, M. S.; Higuchi, T. Prediction of short-term cardiovascular events using quantification of global myocardial flow reserve in patients referred for clinical ^{82}Rb PET perfusion imaging. *J. Nucl. Med.* **2011**, *52*, 726−732.
(84) Merhige, M. E.; Breen, W. J.; Shelton, V.; Houston, T.; D'Arcy, B. J.; Perna, A. F. Impact of myocardial perfusion imaging with PET and ^{82}Rb on downstream invasive procedure utilization, costs, and outcomes in coronary disease management. *J. Nucl. Med.* **2007**, *48*, 1069−1076.
(85) Nandalur, K. R.; Dwamena, B. A.; Choudhri, A. F.; Nandalur, M. R.; Carlos, R. C. Diagnostic performance of stress cardiac magnetic resonance imaging in the detection of coronary artery disease: A meta-analysis. *J. Am. Coll. Cardiol.* **2007**, *50*, 1343−1353.
(86) de Jong, M. C.; Genders, T. S. S.; van Geuns, R.-J.; Moelker, A.; Hunink, M. G. M. Diagnostic performance of stress myocardial perfusion imaging for coronary artery disease: A systematic review and meta-analysis. *Eur. Radiol.* **2012**, *22*, 1881−1895.
(87) Schinkel, A. F.; Poldermans, D.; Elhendy, A.; Bax, J. J. Assessment of myocardial viability in patients with heart failure. *J. Nucl. Med.* **2007**, *48*, 1135−1146.
(88) Ghosh, N.; Rimoldi, O. E.; Beanlands, R. S.; Camici, P. G. Assessment of myocardial ischaemia and viability: Role of positron emission tomography. *Eur. Heart J.* **2010**, *31*, 2984−2995.
(89) Schinkel, A. F.; Bax, J. J.; Poldermans, D.; Elhendy, A.; Ferrari, R.; Rahimtoola, S. H. Hibernating myocardium: Diagnosis and patient outcomes. *Curr. Probl. Cardiol.* **2007**, *32*, 375−410.
(90) Vom Dahl, J.; Eitzman, D. T.; al-Aouar, Z. R. Relation of regional function, perfusion, and metabolism in patients with advanced coronary artery disease undergoing surgical revascularization. *Circulation* **1994**, *90*, 2356−2366.
(91) Kim, R. J.; Fieno, D. S.; Parrish, T. B.; Harris, K.; Chen, E. L.; Simonetti, O. Relationship of MRI delayed contrast enhancement to irreversible injury, infarct age, and contractile function. *Circulation* **1999**, *100*, 1992−2002.
(92) Klein, C.; Nekolla, S. G.; Bengel, F. M.; Momose, M.; Sammer, A.; Haas, F. Assessment of myocardial viability with contrast enhanced magnetic resonance imaging: Comparison with positron emission tomography. *Circulation* **2002**, *105*, 162−167.
(93) Makowski, M. R.; Ebersberger, U.; Nekolla, S.; Schwaiger, M. In vivo molecular imaging of angiogenesis, targeting $\alpha_v\beta_3$ integrin expression, in a patient after acute myocardial infarction. *Eur. Heart J.* **2008**, *29*, 2201.